Materials and Structures (2024) 57:108
https://doi.org/10.1617/s11527-024-02384-0

ORIGINAL ARTICLE

Early-age hydration of ye'elimite (calcium sulfoaluminate phase) in presence of alkalis: role of calcium sulfate

Bipina Thaivalappil · Vaishnav Kumar Shenbagam · Piyush Chaunsali

Received: 23 October 2023 / Accepted: 30 April 2024

Abstract Calcium sulfoaluminate-belite (CSAB) cement is considered a viable and environmentally friendly alternative to Portland cement. Ye'elimite or calcium sulfoaluminate which is the primary phase of CSAB cement undergoes rapid hydration, leading to the formation of ettringite or monosulfate as the major hydration product. The reactivity of ye'elimite can be influenced by other phases (e.g., calcium sulfate, calcium hydroxide, and alkalis) present in CSAB cement, affecting the evolution of hydrated phase assemblage. CSAB cements are known for their useful attributes such as quick setting, early-stage strength development, and the ability to compensate for shrinkage. These properties are directly linked to the early-age hydration of CSAB cement. This study is focused on the influence of alkali and calcium sulfate on the hydration of ye'elimite. Early-age hydration (up to 3 days) of laboratory-synthesized ye'elimite was studied under different alkali concentrations in the mix with or without calcium sulfate. The addition of gypsum was found to accelerate the early-age hydration of ye'elimite, and the alkalis contributed to further acceleration of the hydration in the initial hours. Alkalis were found to stabilize the hydration beyond a few hours, leading to a lower degree of hydration. Furthermore, alkalis influenced the formation as well as morphology of the hydration products, and the influence was more predominant in the absence of gypsum.

Keywords Ye'elimite · Hydration · Alkali · Dissolution · Morphology

1 Introduction

Calcium sulfoaluminate-belite (CSAB) cement is considered as a technically adequate low-CO_2 alternative binder to the conventional Portland cement (PC) for various applications. Prominent characteristics such as rapid strength development, shrinkage compensation, and less energy & CO_2-intensive production led to significant research interest on CSAB cement in the last decade [1–8]. CSAB cements have the potential to reduce the net CO_2 emission by 25–35% compared to PC, depending on their clinker phase composition [9–11]. A reduction in CO_2 emission by up to 55% is possible when industrial wastes or other alternative materials are used to produce CSAB cement [12]. Ye'elimite (Klein's compound or calcium sulfoaluminate phase—$4CaO.3Al_2O_3.SO_3$, $C_4A_3\hat{S}$[1]) constitutes the main phase of CSAB cement. In the 1970s, China started producing CSAB cement commercially under the name 'Third Cement Series (TCS)' [13]. Unlike PC, where CaO

B. Thaivalappil · V. K. Shenbagam · P. Chaunsali (✉)
Department of Civil Engineering, Indian Institute of Technology Madras, Chennai, India
e-mail: pchaunsali@iitm.ac.in

[1] *Cement chemistry notation:* $C = CaO$, $A = Al_2O_3$, $F = Fe_2O_3$, $S = SiO_2$, $\hat{S} = SO_3$.

Published online: 20 May 2024

and SiO_2 dominate the oxide composition, forming alite and belite as major phases, CSAB cements are richer in Al_2O_3, forming ye'elimite as the primary clinker phase. They also contain belite (C_2S), brownmillerite (C_4AF), calcium sulfate ($C\hat{S}$), and other clinker phases. CSAB cement rich in belite phase has now evolved as an intermediate system between the ye'elimite-rich CSAB cement and belite-rich PC and are called belite–ye'elimite–ferrite (BYF) cements or belitic calcium sulfoaluminate (BCSA) cements. Even with the absence of rapid strength-giving phases such as alite (C_3S) and tricalcium aluminate (C_3A), CSAB cement can develop high strengths at early ages due to the presence of ye'elimite.

Hydration of ye'elimite is relatively fast, resulting in rapid setting and early-age strength development in CSAB-based binders. Ye'elimite hydrates in the presence of calcium sulfate, forming predominantly ettringite (AFt) and amorphous aluminium hydroxide (Eq. 1). However, when calcium sulfate depletes, monosulfate (AFm) is also formed (Eq. 2). Ye'elimite hydration with gypsum (as per Eq. 1) requires a water-to-binder ratio (w/b) of at least 0.78 for complete hydration, which raises the water demand in CSAB binders [2]. The ye'elimite phase reacts rapidly if required water and calcium sulfate are available, and complete hydration occurs within the first week [3, 14].

$$C_4A_3\hat{S} + 2\,C\hat{S}H_2 + 34\,H \rightarrow C_3A.3\,C\hat{S}.32\,H + 2\,AH_3 \quad (1)$$

$$C_4A_3\hat{S} + 18\,H \rightarrow C_3A.C\hat{S}.12\,H + 2\,AH_3 \quad (2)$$

As ye'elimite is the primary phase, property development in CSAB-based binders is mainly linked to the hydration of ye'elimite, especially its early strength development and expansion characteristics. However, the hydration characteristics of ye'elimite can be influenced by the presence of other phases. Among the various factors that influence the hydration of ye'elimite, the presence of sulfates and the alkalinity of the reacting solution play a significant role in the reactivity at the early stages of hydration. Alkalis such as Na_2O and K_2O are present in most of the natural raw materials used for cement production. Additionally, in PC-CSAB blended systems, a change in alkalinity due to the presence of PC may bring about different hydration kinetics. The dissolution rate of aluminate phases is found to be higher in the presence of alkalis [15]. Consequently, ye'elimite may show change in reactivity if there is an alkali contribution from the raw materials. Efforts are underway to produce CSAB cement using industrial byproducts. The red mud, used as a partial replacement of bauxite in the CSAB raw mix, is typically highly alkaline in nature as the pH lies between 10 and 13.5 [16]. The early age hydration of CSAB cement was reported to be faster when red mud was used in the production of CSAB clinker due to the contribution of alkalis from red mud [17]. The study by Chen [18] reported an increase in the dissolution of ye'elimite due to higher alkali content in the Class C fly ash and fluidized bed ash (FBA) used for producing the CSAB cement. Only a few studies have attempted to investigate the influence of alkalis on pure ye'elimite [19–21]. Zajac et al. [22], based on a thermodynamic approach, showed that the presence of alkali ions such as potassium raises the ionic strength and the pH, increasing the aluminium ions in the solution, which in turn shifts the solubility curve of ettringite towards a lower calcium and aluminium concentrations. Winnefeld and Barlag [19] reported that the hydration kinetics of ye'elimite could be accelerated by increasing the pH of the reacting medium or by adding calcium sulfate. This study used KOH solutions of molarity 0.01 M and 1 M. Another study by Tambara et al. [23] also reported the acceleration of CSAB cement hydration in a low molarity alkaline solution of NaOH, but a high molarity alkaline solution (> 2 M) retarded the ye'elimite hydration. The major reason for the retardation of hydration was the formation of thenardite from anhydrite and the instability of ettringite at high pH environment [24, 25]. The effect of alkalis can extend from influencing the reactivity of the clinker phases to the morphology of hydration products. Aluminium hydroxide was found to be less crystalline when ye'elimite is hydrated in water or low molarity alkaline solution but showed increased crystallinity with increasing alkalinity of the reacting solution [23, 26]. The available studies on the effect of alkalis in reaction solution on the hydration kinetics of pristine ye'elimite are mainly based on thermodynamic modelling predictions. As the experimental studies are based on CSAB cement or cement clinker with various phase assemblages and sulfate as well as alkali contents, the mechanism of ye'elimite hydration under the influence of alkalis is not well understood. Moreover,

Table 1 Mixture proportions of ye'elimite-gypsum-alkali mixes

Sample name	Phase composition (wt%)			w/b	Alkali solution molarity (M)
	Ye'elimite	Gypsum	Alkali (NaOH, % bwob[a])		
M0A0	100	0	0	0.5	0
M0A1	100	0	1		0.5
M0A2	100	0	2		1
M2A0	64	36	0	0.5	0
M2A1	64	36	1		0.5
M2A2	64	36	2		1

[a]by weight of binder

severe alkalinity introduced in the ye'elimite hydrating system changes the stability of hydration products (e.g. ettringite) and hence results in different hydrate phase assemblage due to the high pH of the aqueous solution. This study attempts to understand the hydration of pure ye'elimite and ye'elimite-gypsum blend in moderate alkali conditions (≤ 1 M) to isolate the effect of alkalis on ye'elimite hydration. This work could contribute to a better understanding of the dissolution kinetics and early-age hydration of ye'elimite under varying sulfate and alkali environments, which is limited in the existing literature. Moreover, the results are expected to have implications on the use of alkali-rich industrial byproducts such as red mud in the CSAB clinker production.

2 Materials and methods

2.1 Raw materials

Pure ye'elimite was synthesized in laboratory scale using laboratory-grade calcium oxide (> 90% CaO), alumina (> 95% Al_2O_3), and calcium sulfate (> 96% $CaSO_4$). Laboratory-grade calcium sulfate dihydrate (> 99% $CaSO_4.2H_2O$) and sodium hydroxide (> 97% NaOH) were used as the sources of gypsum and alkalis, respectively, for the hydration study. Two sets of pastes were prepared at a water-to-binder ratio (w/b) of 0.5: (1) ye'elimite hydrating in the presence of gypsum with varying alkali concentrations, and (2) ye'elimite hydrating in the absence of gypsum with varying alkali concentrations. For ye'elimite hydrating with gypsum, the molar ratio of gypsum-to-ye'elimite (M value) was fixed as M = 2 to ensure a sufficient amount of sulfate for ettringite formation. The mix proportions used in the study are shown in Table 1. The pH of alkali solutions used for A1 and A2 mixes was measured using Metrohm 913 pH meter and was 13.2 and 13.4, respectively.

2.2 Synthesis procedure

2.2.1 Step 1: Proportioning of raw materials

Stoichiometric proportions of the oxides were calculated for the synthesis of pure ye'elimite. As the volatilization of sulfur happens beyond 1200 °C, an additional 5% of $CaSO_4$ was added to the raw mix to compensate for the loss of sulfur and to ensure the maximum yield of ye'elimite during clinkering.

2.2.2 Step 2: Mixing of raw materials and pelletization

In this step, the proportioned raw mix was homogenized by adding water, followed by mixing using a stirrer. The raw mix was kept in the oven at 105 °C for 12 h to remove the water. Further, the mix was pelletized under 1.5 tons in a Controls—250 kN Servo Hydraulic—compression testing machine to facilitate solid-state reactions during clinkering.

2.2.3 Step 3: Sintering and cooling

The raw mix pellets were placed in alumina crucibles and fired in an electric muffle furnace (INDFUR) at a heating rate of 5 °C/min. Once the maximum temperature was attained, the pellets were held at that temperature for a specified period (retention time) to ensure the complete formation of phases. Different maximum temperatures ranging from 1200 to 1400 °C with retention time varying from 1 to 4 h were used to optimize the clinkering conditions to

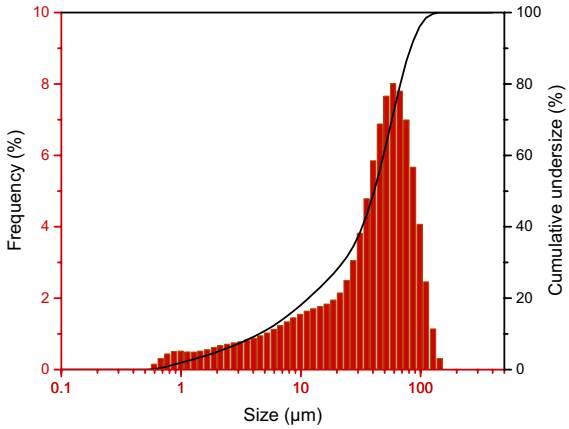

Fig. 1 Particle size distribution of synthesized ye'elimite used in experiments

ensure maximum ye'elimite formation. The clinker was removed from the furnace at 1000 °C, followed by air cooling.

2.2.4 Step 4: Grinding

After cooling to room temperature, the ye'elimite clinker was ground in a planetary ball mill to obtain the required fineness. The particle size distribution of the synthesized ye'elimite after grinding is shown in Fig. 1.

2.3 Sample preparation and test methods

2.3.1 Preparation of paste samples

The ye'elimite pastes were prepared by mixing at 23 ± 2 °C. All the pastes were cast in plastic vials and cured at 23 ± 2 °C under sealed conditions. Stopping hydration is necessary for paste characterization at different ages so that the properties of interest can be preserved and captured effectively. The solvent exchange method [27] was used in the current study to stop the hydration. Small saw-cut slices of paste samples were submerged in a relatively large amount of isopropyl alcohol for three days, with replenishing the isopropyl alcohol after one day. Until testing, all the samples were stored in a vacuum desiccator along with silica gel to remove any moisture present and prevent exposure to ambient air.

Table 2 Phases and collection codes used for XRD analysis

Phase name	Cement chemistry notation	ICSD collection code
Ye'elimite (orthorhombic)	$C_4A_3\check{S}$-o	80361
Ye'elimite (cubic)	$C_4A_3\check{S}$-c	9560
Anhydrite	$C\check{S}$	15876
Calcium monoaluminate	CA	260
Calcium dialuminate	CA_2	16191
Gypsum	$C\check{S}H_2$	409581
Ettringite	AFt	155395
Monosulfate	AFm	100138

2.3.1.1 Particle size distribution

The particle size distribution (PSD) of synthesized ye'elimite was measured using laser diffraction through Malvern Mastersizer MS 3000 equipped with Hydro EV accessory for wet dispersion. Isopropyl alcohol was used as a dispersing medium. Ultrasonication for a duration of 60 s was done to prevent agglomeration of the particles. A refractive index of 1.568 was used for PSD measurements of ye'elimite [28].

2.3.1.2 X-ray powder diffraction

The clinkers were wet ground using an agate mortar and pestle with isopropanol as grinding media to pass through a 75 μm sieve. Hydrated samples were taken for X-ray diffraction (XRD) after hydration stoppage as discussed in Section 2.3 followed by the same micronizing and sieving process. It was ensured that the entire quantity taken for grinding was passed through the 75 μm sieve in order to avoid fractionation of the samples. The phase assemblages of synthesized clinkers and hydrated cements were determined using the X-ray diffractogram obtained from the Rigaku X-ray diffractometer equipped with Cu-Kα radiation tube (λ = 1.5408 Å). The quantitative phase analysis (QXRD) was carried out using Rietveld refinement in PANalytical Xpert High Score Plus Software V.3. For quantifying amorphous phases in hydrated samples, internal standard method was used. Reagent grade ZnO (> 99% purity) was used as an internal standard at a doping level of 20% by mass. The collection codes of the phases used for Rietveld refinement are given in Table 2.

2.3.1.3 Thermogravimetric analysis Thermogravimetric analysis (TGA) was performed on hydrated samples using LABSYS EVO TG–DTA/DSC-1600 °C model equipment under N_2 atmosphere. Approximately 10–15 mg of sample was heated between 50–1000 °C at a heating rate of 10 °C/min.

2.3.1.4 Bound water measurement The amount of non-evaporable water present in the hydrated system gives an estimate of the water that is bound to the hydration products. In order to estimate the bound water content, direct mass loss measured from loss-on-ignition method and mass loss calculated from TG measurements were adopted [27, 29]. The mass loss is typically captured from 105 °C for PC-based systems to calculate bound water [27]. However, the decomposition of ettringite could start at temperatures well below 105 °C [30–33]. To avoid the loss of bound water in ettringite, the weight loss of oven-dried samples from 50 °C onwards was considered to capture the complete decomposition of ettringite during bound water measurement. Sample weighing about 1 g was taken out after hydration stoppage, as explained in Sect. 2.3. The weighed sample was placed in an oven at 50 °C for 12 h, and the weight after drying in the oven was noted. The sample was then placed in a high temperature muffle furnace, heated at 605 °C for 3 h, and further cooled to room temperature. As most of the hydrate phases lose bound water by 605 °C, mass loss between 50 and 605 °C was used as a reasonable approximation of total bound water in the samples. The bound water was calculated as follows using Eq. 3.

$$W_{bw} = \frac{W_{50} - W_{605}}{W_{605}} \quad (3)$$

W_{bw} = weight of bound water (g/g of binder).
W_{50} = weight of sample after heating at 50 °C (g).
W_{605} = weight of sample after heating at 605 °C (g).

2.3.1.5 Isothermal Calorimetry Calmetrix I-Cal HPC isothermal calorimeter with four sample channels was used to measure heat evolution during the hydration of ye'elimite. Paste samples were mixed externally for 3 min and placed inside the calorimeter in respective channels. The heat was measured against a standard reference mass placed inside the calorimeter. In order to avoid heat evolution during external mixing and to allow the samples to stabilize at the calorimeter set temperature of 23 °C, data from the initial 30 min was not considered for analysis.

2.3.1.6 Scanning electron microscopy The hydrated samples of three days of age were used for secondary electron (SE) imaging using scanning electron microscopy (SEM). After the hydration stoppage, the samples were stored in a vacuum desiccator for at least 24 h with silica gel to absorb any moisture present and to prevent further hydration and/or carbonation. Gold sputter coating was carried out on the sample surface to make it conductive before imaging. Images were captured under a voltage of 5 kV in Zeiss Evo 18 at 2500×, 5000×, and 10,000× magnifications. The distribution and morphology of the phases were observed through SEM images.

2.3.1.7 Inductively coupled plasma optical emission spectroscopy Pure ye'elimite and ye'elimite-gypsum mixes were dissolved in deionized water and alkali solution with a liquid-to-solid ratio of 10. The mixes were kept under continuous dissolution for 6 h using a test tube rotator. After 6 h, the filtered solution was collected using a 0.20 µm size syringe filter and immediately diluted in 1 (filtered solution): 9 (acid) parts using 6.9% HNO_3 solution. The diluted solution was taken for composition analysis using inductively coupled plasma optical emission spectroscopy (ICP-OES), where plasma is used as a high-temperature atomization source. The analyte atoms were atomized by the plasma, and the characteristic spectra emitted by the atoms were used to identify and quantify them.

3 Results

3.1 Clinkering and formation of phases

Different clinkering pathways were followed by changing maximum temperatures and retention times. The X-ray diffractograms of the synthesized clinkers are shown in Fig. 2. The yield of ye'elimite was observed to be high when the maximum synthesis temperature was above 1300 °C, without significant amounts of secondary phases such as CA and CA_2. Below 1300 °C, some part of calcium sulfate remained unreacted, and hence ye'elimite was

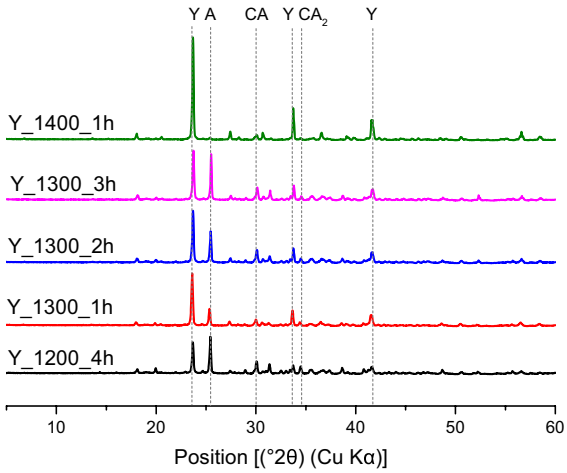

Fig. 2 X-ray diffractograms of ye'elimite synthesized using pelletized raw mix. *Note:* Sample name indicates Ye'elimite_ Maximum temperature in °C _Retention time, Y: Ye'elimite, A: Anhydrite, CA: Calcium mono aluminate, CA_2: Calcium dialuminate

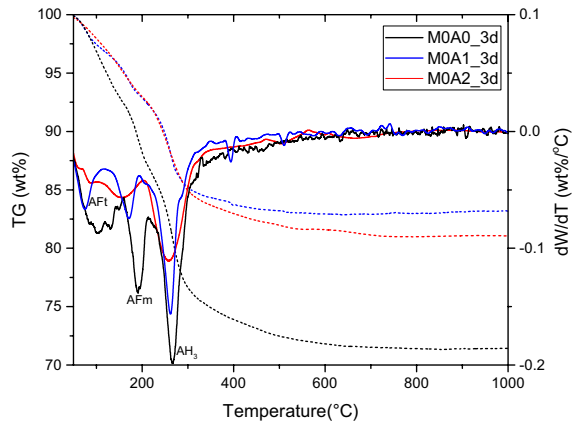

Fig. 3 Thermogravimetric analysis of 3 day hydrated ye'elimite (in the absence of gypsum at different alkali dosages)

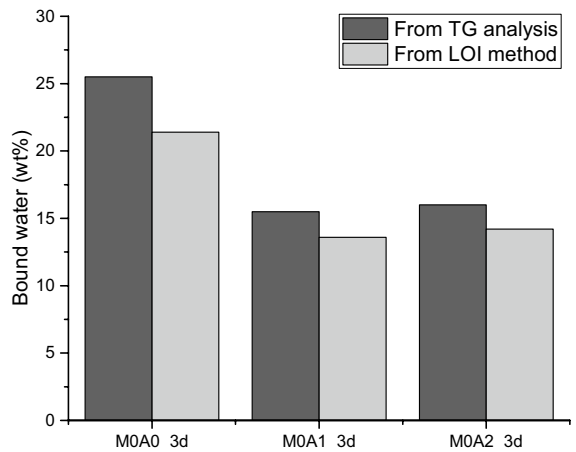

Fig. 4 Bound water for 3 day hydrated ye'elimite in the absence of gypsum with different alkali dosages

not completely formed. The ye'elimite synthesized at 1400 °C with 1 h retention time contained 94.8% ye'elimite along with 2.4% calcium sulfate and some minor phases. The yield was observed to be maximum at 1400 °C, though literature reports the formation of ye'elimite below this temperature, between 1200 to 1300 °C [5]. It is noted that higher temperatures were crucial for complete ye'elimite formation rather than longer retention times at lower temperatures. However, the effect of clinkering conditions on the formation of ye'elimite was not explored in detail in this work. A maximum temperature of 1400 °C and retention time of 1 h were used for the synthesis of ye'elimite that was used in all the tests in this study.

3.2 Hydration reactions and hydrate phase evolution

Early-age hydration of ye'elimite was studied using XRD and TG analyses. Figure 3 shows the cumulative and derivative mass loss from TG of the pure ye'elimite mixes hydrated for three days in the absence of gypsum, with varying amounts of alkalis in the reacting solution. Monosulfate (AFm, mass loss in the range of 150–200 °C) and aluminium hydroxide (AH_3, mass loss in the range of 200–300 °C) were identified as the major hydration products of pure ye'elimite in the absence of calcium sulfate [2]. From Fig. 3, it can be noted that there was a decrease in the amount of hydrate in the presence of alkalis in the mixes without gypsum, as there was a reduction in the cumulative mass loss. However, there was no significant difference between the hydration of mixes containing 1% and 2% of alkali. As no gypsum was present in the mixes, the cumulative mass loss curve could be directly correlated to the bound water and the degree of hydration. The bound water calculated from the TG plot as well as from the bound water test mentioned in Section 2.3.5 are shown in Fig. 4. The bound water values at three days were similar for both the alkali-containing mixes, but these values were considerably lower for pure ye'elimite without alkali,

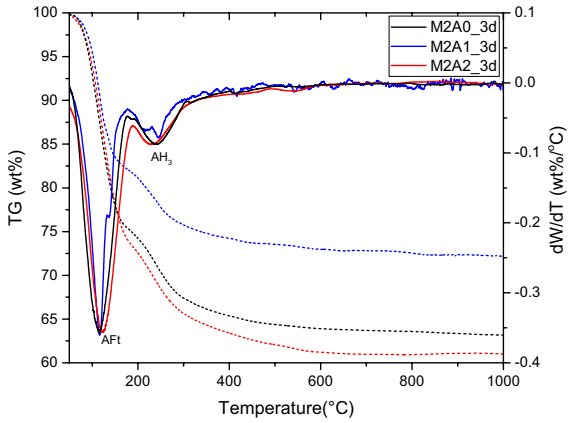

Fig. 5 Thermogravimetric analyses of 3 day hydrated ye'elimite mixes (in presence of gypsum and different alkali dosages)

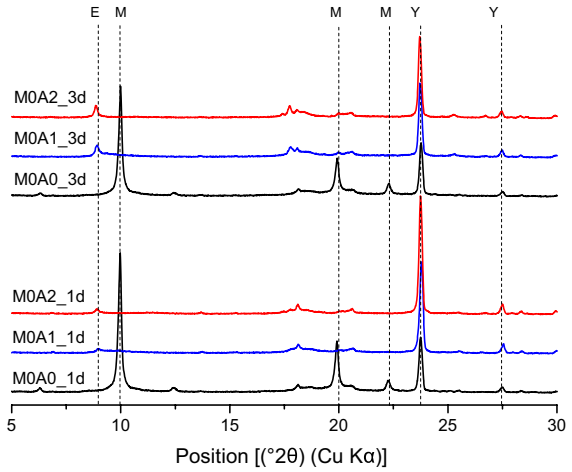

Fig. 6 XRD of 1 and 3 day hydrated ye'elimite in the absence of gypsum: influence of alkali content *(E: Ettringite, M: Monosulfate, G: Gypsum, Y: Ye'elimite)*

indicating a reduced degree of hydration. Additionally, the bound water values associated with AFm phase in M0A0, M0A1, and M0A2 were 9.95, 5.59, and 4.38%, respectively. Whereas the same for AH_3 phase was 8.88, 7.50, and 8.45%, respectively. While the bound water in AH_3 phase remains comparable in the three systems, the reduction in total bound water can be mainly attributed to AFm phase. This is an indication that the precipitation of AFm phase may be suppressed in the presence of alkali, whereas AH_3 formation is not affected as much.

Ettringite (mass loss in the range of 50–150 °C) and aluminium hydroxide were the main hydration products when ye'elimite reacts in the presence of gypsum [2]. In the hydrated mix having ye'elimite and gypsum, DTG peaks corresponding to ettringite and aluminium hydroxide overlapped for the 2% alkali mix and 0% alkali mix (Fig. 5). In the 1% alkali mix, a shoulder peak attributed to the loss of water from gypsum and can be seen at ~ 150 °C. The expected monosulfate formation is minimal in the mixes as they contain sufficient amounts of gypsum (M = 2) to favour the ettringite formation during ye'elimite hydration. However, the presence of monosulfate (if any) could not clearly be distinguished in TG plot due to peak overlapping. The cumulative mass loss was similar in the 0% alkali and 2% alkali mixes, whereas it was reduced in the 1% alkali mix. As the cumulative mass loss from TG is not only corresponding to the bound water from hydration products but also from the gypsum that could be remaining in the mix, it was difficult to predict the extent of hydration based only on TG. Hence, XRD was used to derive the hydrated phase assemblage.

The XRD patterns of the ye'elimite-alkali mixes without gypsum are shown in Fig. 6. In the 0% alkali mix (M0A0_3d), monosulfate in the form of crystalline kuzelite (ICSD 100138) was identified as the major hydration product, which was not evident in the alkali-containing mixes (M0A1_3d and M0A2_3d). Monosulfate and aluminium hydroxide were difficult to get detected and quantified through XRD as they generally appear with less crystallinity in ye'elimite-based system [34, 35]. Hence, the total amorphous content along with other hydrates were quantified using Rietveld refinement (see Fig. 8). In the absence of gypsum, the total hydration products decreased in the presence of alkalis in the reaction solution, which was also evident by the higher fraction of unreacted ye'elimite in the hydrating system.

Interestingly, small amounts of ettringite were observed to form even in the absence of gypsum in the alkali-containing ye'elimite mixes, which is also evident from the diffractogram in Fig. 6 and QXRD results in Fig. 8. This could be due to the preferential precipitation of ettringite over monosulfate in the presence of alkali. However, due to the undersaturation with respect to sulfate in the system, ettringite precipitation was limited, further leading to the formation of monosulfate.

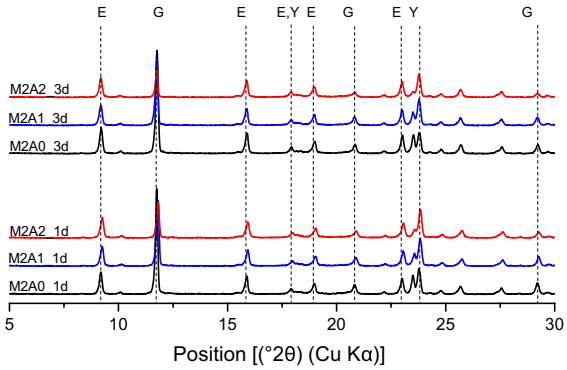

Fig. 7 XRD of 1 and 3 day hydrated ye'elimite in presence of gypsum: influence of alkali content *(E: Ettringite, G: Gypsum, Y: Ye'elimite)*

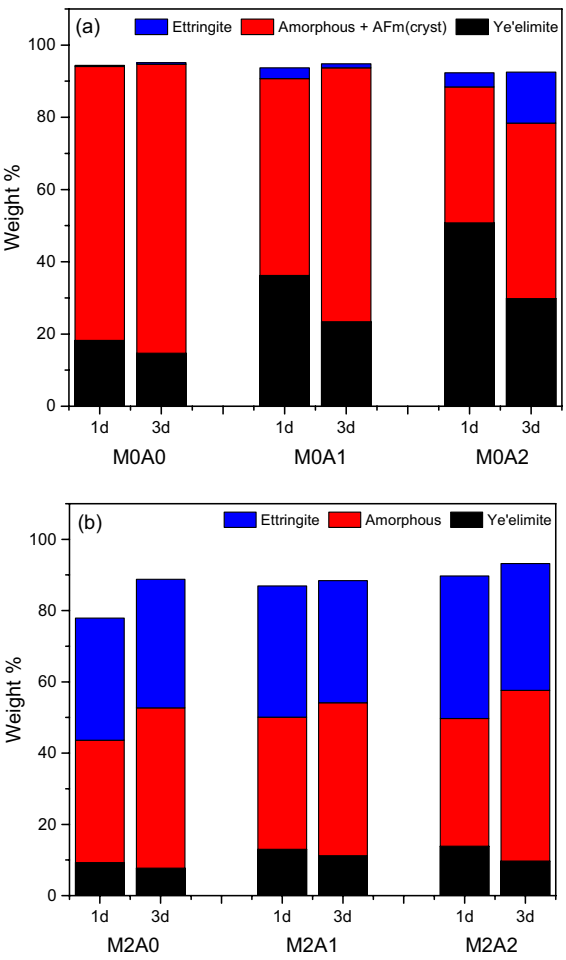

Fig. 8 Major hydrate phases and unhydrated ye'elimite, quantified using QXRD, at 1 and 3 day in ye'elimite hydrated in the **a** absence of gypsum **b** presence of gypsum

In the presence of gypsum, ettringite was the main hydration product along with amorphous hydration products (Fig. 7). The amorphous part was mainly contributed by aluminium hydroxide formed from ye'elimite hydration. The amorphous aluminium hydroxide could not be detected in XRD. The diffractograms didn't show a significant difference in the phase assemblage with the increase in alkali content. As seen from the XRD patterns and QXRD results shown in Fig. 8, the amount of total hydration products didn't reduce significantly in the presence of alkalis in the gypsum containing ye'elimite pastes after 1 day. There was a slight reduction in the hydration at the age of 3 days in 1% alkali mix but the mixes with 0% alkali and 2% alkali behaved similarly.

3.3 Dissolution and hydration kinetics

Isothermal calorimetry was conducted on the paste samples to understand the effect of calcium sulfate and alkalis on ye'elimite hydration kinetics. The addition of gypsum to pure ye'elimite resulted in an acceleration of hydration. The reactivity of ye'elimite is enhanced in the presence of calcium sulfate [19, 36]. In Fig. 9, the hydration peak of gypsum-containing ye'elimite mix (M2A0) was shifted towards the left when compared to the pure ye'elimite (M0A0) hydration peak, resulting in a shortening of the dormant period. But when the alkalis were introduced in these mixes, there was further acceleration of very early-age hydration. As the first 30 min of data were not considered in the analysis due to external missing, the beginning of the major hydration peak in the alkali-containing mixes could not be well captured, which might have affected the total cumulative heat as well. However, a prominent shift in reactions might have taken place during early hydration due to the presence of alkalis; especially in the gypsum-containing mixes, the major peak appeared very early (before 2 h) with a significantly higher heat rate compared to the pure ye'elimite mix without gypsum. This could be attributed to the faster dissolution kinetics of constituents (ye'elimite and gypsum) and possible precipitation of ettringite [23]. However, beyond 10 h, the total heat released in the case of alkali-containing mixes was almost stabilized, showing minimal progress in the further hydration. Hence, the total heat released beyond this period is less than the mixes hydrated without alkali. In the case of mixes without

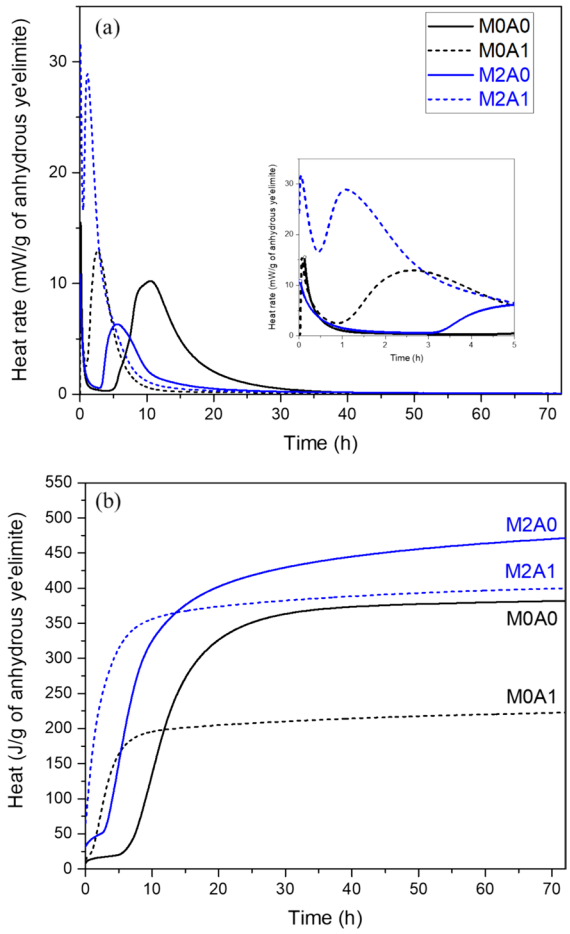

Fig. 9 **a** Heat evolution rate and **b** total heat released in ye'elimite hydrating with and without gypsum with different alkali concentrations in reacting solution.

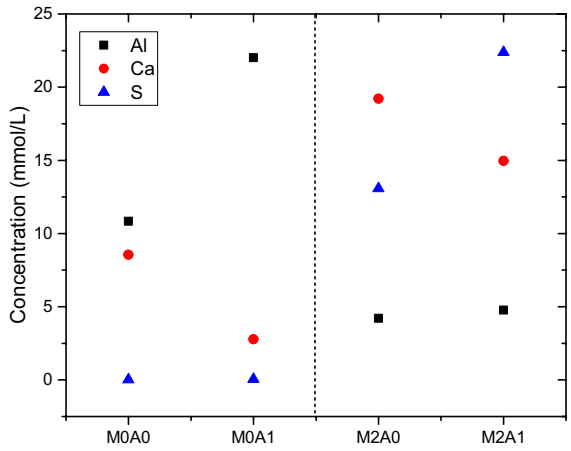

Fig. 10 Concentrations of Al, Ca, S in solution extracted after 6 h of dissolution

gypsum, the difference was more, which is similar to the observations from XRD, TG, and bound water tests. Sánchez-Herrero et al. [37] reported similar observations when ye'elimite hydrated with 4% Na_2CO_3 in an aqueous solution having a pH of 11.75. Previous works by Padilla-Encina et al. [24, 25], also observed a slower progression of hydration in the initial three days when CSA clinker was hydrated in 1 M NaOH solution without the presence of calcium sulfate or gypsum. In the present work, a heat flow was observed around 3 h. Further, only a minimal heat evolution was captured until 72 h, resulting in a reduced cumulative heat in M0A1 compared to M0A0. It may be noted that the composition of the material and particle size in these studies are quite different from that of the present work, which might have resulted in the changes in the observations related to the hydration reactions.

A dissolution study was conducted to understand the influence of alkalis on the dissolution kinetics of ye'elimite in different sulfate environments. The mixes M0A0, M0A1, M2A0, and M2A1 (refer to Table 1 for the mix proportions) were kept in continuous dissolution for 6 h with a liquid-to-solid ratio of 10. Alkali dosage of only 1% was used for dissolution as 2% dosage behaved similar to 1%. The concentration of different ions in the filtered solution measured using ICP-OES is shown in Fig. 10. It can be noted that the addition of NaOH increased the Al concentration in the mix, which had only ye'elimite. The higher Al concentration could be due to the increased solubility of ye'elimite in the presence of alkalis. However, the Ca concentration was slightly decreased in the alkali mix. In contrast, the S concentration remained negligible. When gypsum was present, the Ca, Al and S concentrations in the solution were completely different. The Al concentration reduced significantly (due to the dilution effect with the addition of calcium sulfate) as compared to the no-gypsum mixes, whereas the Ca and S concentrations increased (with the additional source of calcium and sulfate from gypsum). However, the Al concentration remained similar irrespective of the alkali addition in the ye'elimite-gypsum mix. Whereas the S concentration was significantly increased in the presence of alkalis. This indicates that the gypsum dissolved at a faster rate than ye'elimite in the presence of NaOH,

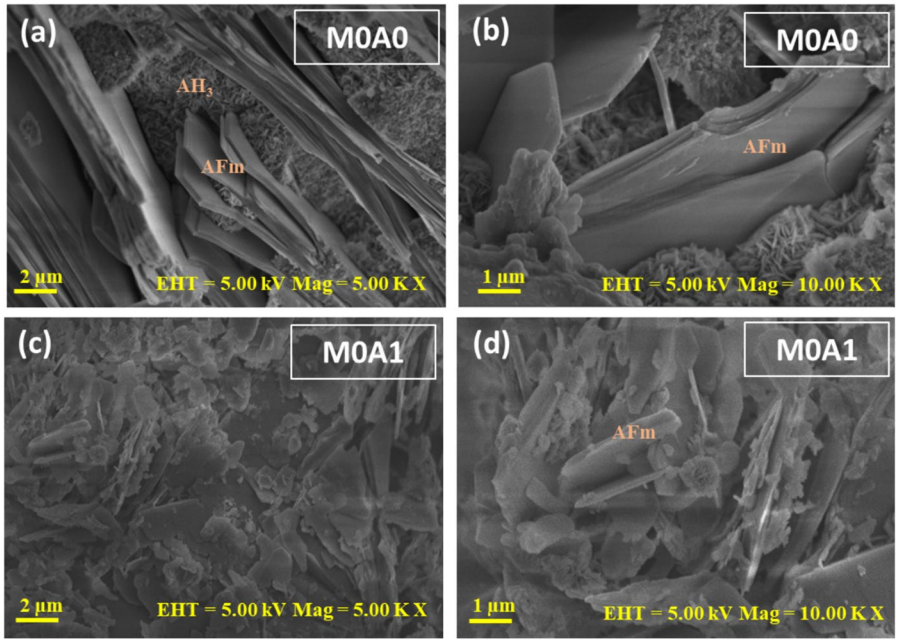

Fig. 11 The microstructure captured in SE imaging in SEM for 3 day hydrated ye'elimite **a–b** without alkali and **c–d** with alkali (in the absence of gypsum)

leading to a higher concentration of Ca and S, and a reduced concentration of Al. The faster dissolution kinetics coupled with the initial precipitation of ettringite can be linked to the early occurrence of the major peak with increased heat rate observed from calorimetry in the ye'elimite-gypsum mix in the presence of alkali, as compared to the alkali-free system.

3.4 Microstructure development

The microstructure development of hydrated ye'elimite was captured using SE imaging in SEM. A noticeable change in the microstructure was observed when ye'elimite hydrated without gypsum in the presence of alkali (Fig. 11). Without the alkali content, a more compact microstructure with monosulfate and aluminium hydroxide was formed. The aluminium hydroxide had a grassy-like fibrillar appearance and precipitated between the hexagonal monosulfate. Other authors have also reported different morphologies confirmed through SEM, including spherical, fibrillar, and lamellar [26, 38]. In the presence of 1% alkali, the microstructure appeared less dense and grassy-like appearance of aluminium hydroxide and hexagonal sheets of monosulfate couldn't be found. This might be due to the reduced degree of hydration of ye'elimite in the alkali-containing mix and also the change in morphology of aluminium hydroxide with pH (increase in pH with the addition of alkalis) [19]. The SEM images of 3 day hydrated ye'elimite in the presence of gypsum are shown in Fig. 12. A change in the morphology of ettringite could be observed from the SE images. In the presence of 1% alkali, a greater number of slender ettringite crystals could be observed as compared to thicker columnar ettringite in the system with no alkali. The change in morphology may be due to the increase in pH of the pore solution and the rapid formation of ettringite. According to [39, 40], the length-to-thickness ratio of ettringite crystals is hugely dependent on reaction solution pH. An increase in OH^- ions in pore solution, leading to increased pH, could facilitate more ettringite crystal nuclei formation, changing the crystal morphology from columnar to fine needle-like rods [40].

4 Discussion

The influence of alkalis on early-age hydration of ye'elimite in the presence and absence of gypsum was studied in the present work. It was well established by prior studies that the gypsum could accelerate the hydration of ye'elimite and contribute to the formation of ettringite, which is crucial for early strength development and shrinkage compensation properties in the ye'elimite-based admixtures and

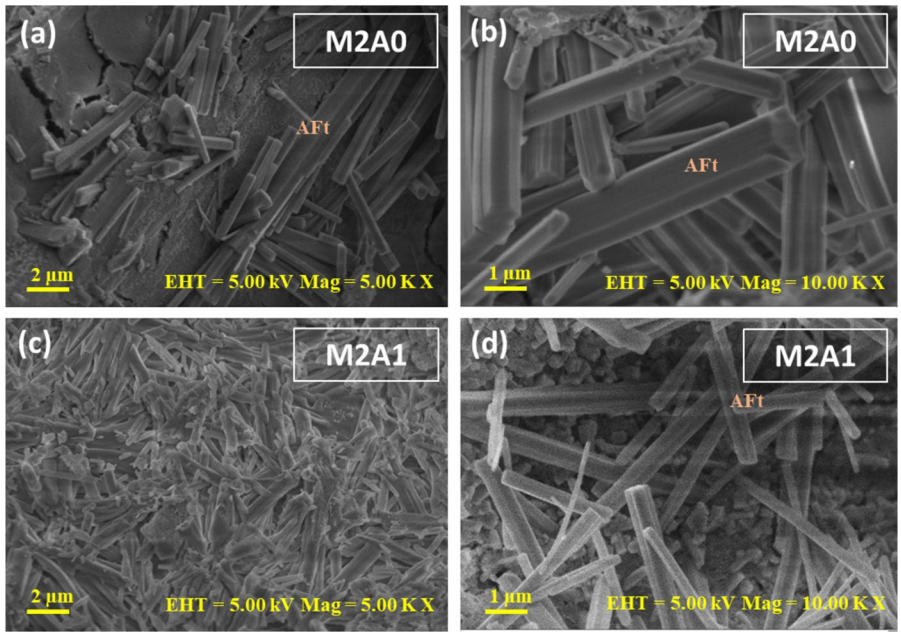

Fig. 12 The microstructure captured in SE imaging in SEM for 3 day hydrated ye'elimite **a–b** without alkali and **c–d** with alkali (in the presence of gypsum)

cements. However, the main objective of this study was to address the question: what is the role of alkalis on ye'elimite hydration taking place in different sulfate environments? To answer this question, a suite of ye'elimite mixes with/without gypsum and incorporating 0–2% alkalis were considered for the study. These mixes were hydrated and assessed for dissolution, hydration reactions, hydration kinetics, and microstructure development using different techniques, including XRD, TG, SEM, ICP_OES, and calorimetry.

The presence of alkalis was found to influence the dissolution of ye'elimite and calcium sulfate. Along with increasing the pore solution's pH, Al, Ca and S concentrations were also altered in the presence of alkalis. The influence of the alterations in pore solution composition was evident on the hydration kinetics, the morphology, and the hydrated phase assemblages.

The presence of alkalis enhanced early-age dissolution of ye'elimite and gypsum, which was evident by a decrease in the dormant period (in addition to the reduction due to the influence of gypsum) as observed in heat flow curves from isothermal calorimetry. This increase was observed to be more favoured towards the dissolution of gypsum than ye'elimite as observed by ICP-OES from the increased amount of sulfur compared to aluminium ions in the solution. However, the effect of alkalis on the later age (beyond 10 h) was found to reduce or slow down the degree of hydration, which was more evident in the pure ye'elimite mixes without gypsum.

The hydrate phase assemblage at 1 day and/or 3 day hydrated pastes characterized through XRD and TG also showed a lower degree of hydration in the presence of alkalis in pure ye'elimite; however, this effect was not much pronounced when gypsum was present. A similar observation was found in a previous study [41], where the NaOH and Na_2SO_4 accelerated the early age hydration kinetics of alite, white cement, and white cement-slag blended system in the first few hours; however, the progress of hydration was slower in the later ages in the presence of alkalis. The lowered degree of hydration was partly attributed to the inhibiting effect of increased Al concentration in the alkali-containing system on silicate species' solubility. In the present work, the precipitation of monosulfate was found to be suppressed in the presence of alkali, even when aluminium hydroxide formation was not seriously affected, which led to a reduced degree of hydration. Small amounts of ettringite precipitation were observed in ye'elimite hydrated in the presence of alkalis, without gypsum. Though it is reported to form ettringite in the presence of 'excess' water even when there is no additional sulfate source [40], it may not be possible in the

present case as the w/b was 0.5, which is lower than the theoretical water demand for complete the hydration of ye'elimite. The presence of alkali increases ionic strength as well as the pH of the reacting solution, resulting in a shift of the ettringite solubility line to lower Ca and Al concentrations [22]. However, the undersaturation with respect to sulfate limited the ettringite precipitation to small amounts.

The alkali's influence is more evident in the formation of monosulfate than ettringite. In the presence of gypsum, alkalis did not have much impact on the degree of hydration to a great extent as ettringite continued to form with a sufficient amount of sulfate available in the system. The effect of the change in pH and the dissolution kinetics is also evident in the morphology of the hydrated products. The SEM micrographs showed a clear distinction in the nature (morphology) of aluminium hydroxide and monosulfate formed in the absence and presence of alkalis. The presence of alkalis in the system affected the overall distribution of hydrate phases and ettringite morphology.

5 Conclusions

The main conclusions drawn from the current study are summarized below.

- Alkali incorporation in both the pure ye'elimite and ye'elimite-gypsum mix resulted in faster hydration kinetics in the initial 10 h, beyond which the rate of heat evolution was plateaued. The influence of alkali in the initial 3 days of hydration was more predominant in the case of pure ye'elimite without an additional sulfate source.
- In the presence of alkali, ettringite formation was preferred over monosulfate even in the absence of an additional sulfate source. The monosulfate formation was suppressed to some extent, and small amounts of ettringite formation were observed in ye'elimite hydrated in the absence of gypsum.
- The acceleration of ye'elimite hydration in the presence of alkalis was more pronounced in the presence of gypsum, as the alkalis contributed to a significantly higher heat rate from the main hydration peak due to the faster dissolution of constituents and precipitation of ettringite. Dissolution of gypsum was much faster in the presence of alkali compared to that of ye'elimite.
- The effect of 1% addition and 2% addition of alkalis had comparable effects on early hydration of ye'elimite, irrespective of the presence of gypsum.
- The morphology and distribution of aluminium hydroxide and monosulfate were affected by the presence of alkalis. In the ye'elimite hydrated with gypsum, the alkalis influenced the slenderness of the ettringite needles precipitated.

Acknowledgements The first author gratefully acknowledges the experimental facilities provided by the Department of Civil Engineering of IIT Madras and the Prime Minister's Research Fellowship from the Ministry of Education, India. The authors would like to acknowledge the Centre of Excellence on Technologies for Low-Carbon and Lean Construction at IIT Madras.

Authors contributions Bipina Thaivalappil: Investigation, Methodology, Formal analysis, Writing-Original Draft. Vaishnav Kumar Shenbagam: Investigation, Methodology, Writing-Original Draft. Piyush Chaunsali: Conceptualization, Writing-Reviewing and Editing, Supervision, Funding acquisition.

Data availability Data will be made available upon the request.

Declarations

Conflict of interest The author(s) declare no conflicts of interest related to the research, authorship, and/or publication of this article.

Ethical approval Not applicable.

References

1. Chen IA, Juenger MCG (2011) Synthesis and hydration of calcium sulfoaluminate-belite cements with varied phase compositions. J Mater Sci 46:2568–2577. https://doi.org/10.1007/s10853-010-5109-9
2. Winnefeld F, Lothenbach B (2010) Hydration of calcium sulfoaluminate cements—experimental findings and thermodynamic modelling. Cem Concr Res 40:1239–1247. https://doi.org/10.1016/j.cemconres.2009.08.014
3. Shenbagam VK, Cepuritis R, Chaunsali P (2021) Influence of exposure conditions on expansion characteristics of lime-rich calcium sulfoaluminate-belite blended cement. Cem Concr Compos 118:103932. https://doi.org/10.1016/j.cemconcomp.2021.103932
4. Guo X, Shi H, Hu W, Wu K (2014) Durability and microstructure of CSA cement-based materials from MSWI fly ash. Cem Concr Compos 46:26–31. https://doi.org/10.1016/j.cemconcomp.2013.10.015

5. El Khessaimi Y, El Hafiane Y, Smith A (2019) Examination of ye'elimite formation mechanisms. J Eur Ceram Soc 39:5086–5095. https://doi.org/10.1016/j.jeurceramsoc.2019.07.042
6. Li L, Wang R, Zhang S (2019) Effect of curing temperature and relative humidity on the hydrates and porosity of calcium sulfoaluminate cement. Construct Build Mater 213:627–636. https://doi.org/10.1016/j.conbuildmat.2019.04.044
7. Canbek O, Erdoğan ST (2020) Influence of production parameters on calcium sulfoaluminate cements. Constr Build Mater 239:117866. https://doi.org/10.1016/j.conbuildmat.2019.117866
8. Chaunsali P (2015) Early-age hydration and volume change of calcium sulfoaluminate cement-based binders. PhD Thesis. University of Illinois.
9. Miller SA, John VM, Pacca SA, Horvath A (2018) Carbon dioxide reduction potential in the global cement industry by 2050. Cem Concr Res 114:115–124. https://doi.org/10.1016/j.cemconres.2017.08.026
10. Chaunsali P, Vaishnav SK (2020) Calcium sulfoaluminate-belite cements: opportunities and challenges. Indian Concr J 94:18–25
11. Hanein T, Galvez-martos J, Bannerman MN (2018) Carbon footprint of calcium sulfoaluminate clinker production. J Clean Prod 172:2278–2287. https://doi.org/10.1016/j.jclepro.2017.11.183
12. Sharma A, Basavaraj AS, Chaunsali P, Gettu R (2023) Calcium sulfoaluminate cement manufacturing in india—prospects and prognosis of environmental impacts. ACI Mater J 120:17–28. https://doi.org/10.14359/51738456
13. Gartner E (2004) Industrially interesting approaches to "low-CO2" cements. Cem Concr Res 34:1489–1498. https://doi.org/10.1016/j.cemconres.2004.01.021
14. Kasselouri V, Tsakiridis P (1995) A study on the hydration products of a non-expansive sulfoaluminate cement. Cem Concr Res 25:1726–1736. https://doi.org/10.1016/0008-8846(95)00168-9
15. Jawed I, Skalny J (1978) Alkalies in cement: a review ii. effects of alkalies on hydration and performance of portland cement. Cem Concr Res 8:37-51. https://doi.org/10.1016/0008-8846(78)90056-X
16. Ribeiro DV, Labrincha JA, Morelli MR (2011) Potential use of natural red mud as pozzolan for Portland cement. Mater Res 14:60–66. https://doi.org/10.1590/S1516-14392011005000001
17. Canbek O, Shakouri S, Erdoğan ST (2020) Laboratory production of calcium sulfoaluminate cements with high industrial waste content. Cem Concr Compos 106:103475. https://doi.org/10.1016/j.cemconcomp.2019.103475
18. Chen IA (2009) Synthesis of Portland Cement and Calcium Sulfoaluminate-Belite Cement for Sustainable Development and Performance. PhD Thesis. The University of Texas at Austin.
19. Winnefeld F, Barlag S (2010) Calorimetric and thermogravimetric study on the influence of calcium sulfate on the hydration of ye'elimite. J Therm Anal Calorim 101:949–957. https://doi.org/10.1007/s10973-009-0582-6
20. Ogawa K, Roy DM (1982) C4A3$̄$ hydration, ettringite formation, and its expansion mechanism: III. Effect of CaO, NaOH and NaCl; conclusions. Cem Concr Res 12:247–256. https://doi.org/10.1016/0008-8846(82)90011-4
21. Palou MT, Majling J (1996) Effects of sulphate, calcium and aluminum ions upon the hydration of sulphoaluminate belite cement. J Therm Anal 46:549–556. https://doi.org/10.1007/BF02135034
22. Zajac M, Skocek J, Bullerjahn F, Lothenbach B, Scrivener K, Ben Haha M (2019) Early hydration of ye'elimite: insights from thermodynamic modelling. Cem Concr Res 120:152–163. https://doi.org/10.1016/j.cemconres.2019.03.024
23. Tambara LUD, Cheriaf M, Rocha JC, Palomo A, Fernández-Jiménez A (2020) Effect of alkalis content on calcium sulfoaluminate (CSA) cement hydration. Cem Concr Res 128:105953. https://doi.org/10.1016/j.cemconres.2019.105953
24. Padilla-Encinas P, Palomo A, Blanco-Varela MT, Fernández-Jiménez A (2020) Calcium sulfoaluminate clinker hydration at different alkali concentrations. Cem Concr Res 138:106251. https://doi.org/10.1016/j.cemconres.2020.106251
25. Padilla-Encinas P, Fernández-Carrasco L, Palomo A, Fernández-Jiménez A (2022) Effect of alkalinity on early-age hydration in calcium sulfoaluminate clinker. Cem Concr Res 155:106781. https://doi.org/10.1016/j.cemconres.2022.106781
26. Zhang Y, Chang J (2018) Microstructural evolution of aluminum hydroxide gel during the hydration of calcium sulfoaluminate under different alkali concentrations. Constr Build Mater 180:655–664. https://doi.org/10.1016/j.conbuildmat.2018.06.010
27. Scrivener K, Snellings R, Lothenbach B (eds) (2016) A Practical Guide to Microstructural Analysis of Cementitious Materials. CRC Press (1st Edition). https://doi.org/10.1201/b19074
28. Hawthorne FC, Bladh KW, Burke EAJ, et al. (1987) New mineral names. Am Mineral 72:222–230. https://doi.org/10.2138/am-2018-NMN103234
29. Snellings R, Chwast J, Cizer Ö et al (2018) Report of TC 238-SCM: hydration stoppage methods for phase assemblage studies of blended cements—results of a round robin test. Mater Struct 51:111. https://doi.org/10.1617/s11527-018-1237-5
30. Taylor HFW, Famy C, Scrivener KL (2001) Delayed ettringite formation. Cem Concr Res 31:683–693. https://doi.org/10.1016/S0008-8846(01)00466-5
31. Ogawa K, Roy DM (1981) C4A3S hydration ettringite formation, and its expansion mechanism: I. expansion; Ettringite stability. Cem Concr Res 11:741–750. https://doi.org/10.1016/0008-8846(81)90032-6
32. Zhou Q, Glasser FP (2001) Thermal stability and decomposition mechanisms of ettringite at <120°C. Cem Concr Res 31:1333–1339. https://doi.org/10.1016/S0008-8846(01)00558-0
33. Fridrichová M, Dvořák K, Gazdič D, Mokrá J, Kulísek K (2016) Thermodynamic stability of ettringite formed by hydration of ye'elimite clinker. Adv Mater Sci Eng 2016:9280131. https://doi.org/10.1155/2016/9280131
34. Paul G, Boccaleri E, Buzzi L, Canonico F, Gastaldi D (2015) Friedel's salt formation in sulfoaluminate cements: a combined XRD and 27Al MAS NMR study. Cem Concr

Res 67:93–102. https://doi.org/10.1016/j.cemconres.2014.08.004
35. Gastaldi D, Paul G, Marchese L, Irico S, Boccaleri E, Mutke S, Buzzi L, Canonico F (2016) Hydration products in sulfoaluminate cements: evaluation of amorphous phases by XRD/solid-state NMR. Cem Concr Res 90:162–173. https://doi.org/10.1016/j.cemconres.2016.05.014
36. Hargis CW, Kirchheim AP, Monteiro PJM, Gartner EM (2013) Early age hydration of calcium sulfoaluminate (synthetic ye'elimite, C 4A3$\bar{S}$) in the presence of gypsum and varying amounts of calcium hydroxide. Cem Concr Res 48:105–115. https://doi.org/10.1016/j.cemconres.2013.03.001
37. Sánchez-Herrero MJ, Fernández-Jiménez A, Palomo A (2013) C4A3$\bar{S}$ hydration in different alkaline media. Cem Concr Res 46:41–49. https://doi.org/10.1016/j.cemconres.2013.01.008
38. Song F, Yu Z, Yang F, Lu Y, Liu Y (2015) Microstructure of amorphous aluminum hydroxide in belite-calcium sulfoaluminate cement. Cem Concr Res 71:1–6. https://doi.org/10.1016/j.cemconres.2015.01.013
39. Stark J, Bollmann K (2000) Delayed ettringite formation in concrete structures. Nord Concr Res 23:4–28.
40. Zhu Y, Liu Y, Zhang J (2022) Monitoring the hydration behavior of hardened cement paste affected by different environmental pH regimes. Front Mater 9. https://doi.org/10.3389/fmats.2022.980887
41. Gassó BM (2015) Impact of alkali salts on the kinetics and microstructural development of cementitious systems. PhD Thesis (No. 6763). EPFL.